Int. J. Heat Mass Transfer. Vol. 21, pp. 499–509. Pergamon Press 1978. Printed in Great Britain

CONVECTIVE HEAT TRANSFER THROUGH BOUNDARY LAYERS WITH ARBITRARY PRESSURE GRADIENT AND NON-ISOTHERMAL SURFACES

D. R. JENG,* M. H. LEE† and K. J. DEWITT*

(Received 7 March 1977 and in revised form 12 August 1977)

Abstract—The solution method introduced by Chao and Cheema in their study of forced convection wedge flow with non-uniform surface temperature has been generalized to treat general two-dimensional and axisymmetric boundary-layer flows with non-uniform surface temperature. By the introduction of appropriate transformation variables, the equations for the temperature profile and the local wall heat flux can be expressed explicitly in terms of the Prandtl number and the wedge parameter for a step discontinuity in wall temperature. Numerical examples for an isothermal surface and for a wall temperature step change for a circular cylinder are given and are compared with values obtained from other formula available in the literature.

NOMENCLATURE

$a(\xi)$, $f''(\xi, 0)$;
$a_0(\xi)$, $f_0''(\xi, 0)$;
b, $\left[\dfrac{Pra(\xi)}{3!}\right]^{1/3}$;
C, 3/4;
C_p, specific heat for constant pressure;
$\dfrac{dp}{dx}$, streamwise pressure gradient;
D, diameter of circular cylinder;
$l(x-x_0)$, Heaviside unit operator;
$x-x_0 < 0, \quad l(x-x_0) = 0$;
$x-x_0 \geqslant 0, \quad l(x-x_0) = 1$;
k, thermal conductivity;
L, characteristic length;
Nu, Nusselt number, defined by $\dfrac{q_w L}{k(T_w - T_\infty)}$;
Pr, Prandtl number $= C_p\mu/k$;
q, heat flux;
T, temperature;
u, velocity component in x direction;
U, velocity outside of boundary layer;
v, velocity component in y direction;
r, radius of an axisymmetrical body at the point x;
Re_L, Reynolds number $= U_\infty L/\nu$;
Re_D, Reynolds number $= U_\infty D/\nu$;
x, streamwise coordinate measured along surface from forward stagnation point;
x_0, location in x direction where the wall temperature has a discontinuity;
X, transformed dimensionless coordinate defined in (19a);
y, coordinate normal to surface.

Greek symbols

α, thermal diffusivity;
$\Gamma(n)$, gamma function $= \int_0^\infty \alpha^{n-1} e^{-\alpha} d\alpha$;
$\Gamma(n, x)$, incomplete gamma function $= \int_0^x \alpha^{n-1} e^{-\alpha} d\alpha$;
η, dimensionless coordinate defined in (11);
Λ, wedge variable defined in (14);
θ, dimensionless temperature defined in (17);
θ_n, coefficients in series (25);
ζ, transformed coordinate defined in (19b);
μ, dynamic viscosity;
ν, kinematic viscosity;
ξ, transformed dimensionless coordinate defined in (11);
ρ, mass density;
τ_w, wall shear stress.

Subscripts

e, refers to outer edge of boundary layer;
w, refers to wall condition;
∞, refers to free stream condition.

1. INTRODUCTION

THE ANALYSIS of heat transfer through a laminar boundary layer in the flow over a body of arbitrary shape and arbitrarily specified surface temperature constitutes a unique and important problem in the field of heat transfer. The prediction of heat transfer under such conditions encompasses a wide range of technological applications, such as the calculation of heat transfer at the front portions of a projectile, aircraft, or other body moving through the atmosphere, cooling problems in turbine blades, etc.

More than two and a half decades ago, Lighthill [1]

*Departments of Mechanical and Chemical Engineering, The University of Toledo, Toledo, Ohio, U.S.A.
†Presently at the Department of Chemical Engineering, Auburn University, Auburn, Alabama, U.S.A.

obtained an expression for calculating the heat-transfer rate across a laminar incompressible boundary layer past a two-dimensional body for arbitrary distribution of main stream velocity and wall temperature. Using a linear velocity distribution, i.e.

$$u = \frac{\tau_w(x)}{\mu} y.$$

Lighthill obtained a formula relating the heat-transfer rate to the temperature and shear stress distribution along the wall by solving the boundary-layer equations in the Von Mise's form using the Heaviside operational technique. His results for the case of a step discontinuity in surface temperature may be rephrased in the present notation as

$$NuRe_L^{-1/2} = 0.53835 Pr^{1/3}\left(\frac{L}{U_\infty}\right)^{1/2} \times (\rho\mu)^{-1/6}\tau_w^{1/2}\left[\int_{x_0}^{x} \tau_w^{1/2}\,\mathrm{d}x\right]^{-1/3}. \quad (1)$$

Because the velocity profile was assumed linear, Lighthill's formula (1) is only asymptotically correct for large Prandtl number fluids and the region, irrespective of Prandtl number, near the point x_0 where the surface temperature has encountered a step change. Under the above two conditions, the thermal boundary layer is much thinner than the momentum boundary layer, and, therefore, the assumption of a linear velocity profile is valid. Later, by using the integral method, Liepmann [2] generalized (1) for compressible flow and also applied it to the flow near the separation point.

In order to improve the applicability of (1) to fluids with moderate or small Prandtl numbers and for a region where the thermal and the momentum boundary-layer thicknesses are of the same order of magnitude, several researchers have attempted to improve Lighthill's results or to reanalyze the same problem. Sparrow [3] applied the Görtler series to demonstrate that an exact solution for the title problem can be recast in terms of universal functions, which are independent of the wall temperature distribution of a particular problem; however, no numerical results of these universal functions were obtained. In 1957, Spalding [4] employed a quadratic velocity distribution of the form

$$u = \frac{\tau_w(x)}{\mu} y + \frac{1}{2\mu}\frac{\mathrm{d}p}{\mathrm{d}x} y^2 \quad (2)$$

in order to incorporate the effect of the streamwise pressure gradient into the velocity field. Spalding thus obtained an improved expression of Lighthill's results having a correction term which accounts for the departure from linearity of the velocity profile within the thermal boundary layer. The above analysis was based on an integral energy equation and a dimensional analysis technique, and his results in the present notation can be expressed as

$$NuRe_L^{-1/2} = Pr^{1/3}\left(\frac{L}{U_\infty}\right)^{1/2}(\rho\mu)^{-1/6}\tau_w^{1/2} \times \left\{\int_{x_0}^{x}\left[6.41 + F\left(\frac{\Delta_4\delta_4}{\nu}\frac{\mathrm{d}U_e}{\mathrm{d}x}\right)\right]\tau_w^{1/2}\,\mathrm{d}x\right\}^{-1/3}. \quad (3)$$

Based on dimensional analysis and physical reasoning, the function F is shown by Spalding to solely depend upon the curvature parameter, $\Delta_4\delta_4/\nu\,\mathrm{d}U_e/\mathrm{d}x$, ($\delta_4$ is the shear thickness defined as $\delta_4 \equiv U_e/(\partial u/\partial y)_{y=0}$, and Δ_4 is the conduction thickness defined as $\Delta_4 \equiv -T_w/(\partial T/\partial y)_{y=0}$), which is a measure of the importance of the second term on the RHS of the velocity profile (2) with respect to the first term. The function F was presented as a curve vs $\Delta_4\delta_4/\nu\,\mathrm{d}U_e/\mathrm{d}x$, which was obtained by a curve fitting technique using known data for isothermal wedge flow and for a rotating disc. The accuracy of F is therefore questionable and, furthermore, the use of (3) to evaluate the local heat flux involves an iteration procedure and graphical integration.

In 1972, Chao [5] improved Lighthill's results by expressing the solution of the governing energy boundary-layer equation in terms of a sequence of universal functions. By adopting a quadratic velocity distribution as given by (2) and by using a unique coordinate transformation, Chao was able to obtain a series expression which is a perturbation from Lighthill's solution as

$$NuRe_L^{-1/2} = 3^{-2/3}Pr^{1/3}\left(\frac{L}{U_\infty}\right)^{1/2}(\mu\rho)^{-1/6}\tau_w^{1/2} \times\left[\int_{x_0}^{x}\tau_w^{1/2}\,\mathrm{d}x\right]^{-1/3}\cdot\left[-\frac{\partial\theta}{\partial\xi}(X,0)\right] \quad (4a)$$

where

$$\begin{aligned} -\frac{\partial\theta}{\partial\xi}(X,0) &= 1.11985 - 0.18868\varepsilon - 0.07271\varepsilon^2 - 0.05079\varepsilon^3 + \ldots \\ &\quad - 0.05731\frac{\mathrm{d}\varepsilon}{\mathrm{d}X} - 0.03600\varepsilon\frac{\mathrm{d}\varepsilon}{\mathrm{d}X} + \ldots \\ &\quad + 0.09861\frac{\mathrm{d}^2\varepsilon}{\mathrm{d}X^2} + 0.09161\varepsilon\frac{\mathrm{d}^2\varepsilon}{\mathrm{d}X^2} + \ldots \\ &\quad - 0.11358\frac{\mathrm{d}^3\varepsilon}{\mathrm{d}X^3} - 0.10676\varepsilon\frac{\mathrm{d}^3\varepsilon}{\mathrm{d}X^3} + \ldots \\ &\quad + 0.12004\frac{\mathrm{d}^4\varepsilon}{\mathrm{d}X^4} + 0.10557\varepsilon\frac{\mathrm{d}^4\varepsilon}{\mathrm{d}X^4} + \ldots \end{aligned} \quad (4b)$$

in which

$$X = \ln\int_{x_0}^{x}(\tau_w\mu\rho)^{1/2}\,\mathrm{d}x$$

and the perturbation variable

$$\varepsilon = -\frac{\mathrm{d}p}{\mathrm{d}x}\cdot(2\tau_w\rho G)^{-1},$$

where

$$G = 3^{-2/3}Pr^{1/3}\left(\frac{\tau_w}{\rho\mu}\right)^{1/2}\left[\int_{x_0}^{x}(\tau_w\rho\mu)^{1/2}\,\mathrm{d}x\right]^{-1/3}$$

for an incompressible fluid. [The ξ used in (4b) is defined as $\xi = \rho y G$ which is different from the transformation defined in (11).] It can be readily shown that Chao's perturbation variable, ε, is indeed similar to Spalding's curvature parameter, and that they are related by the following expression:

$$\frac{\Delta_4 \delta_4}{\nu} \frac{dU_e}{dx} = 1.7861\varepsilon. \tag{5}$$

When $\varepsilon = 0$, (4) is identical to Lighthill's result (1), and Chao's result therefore presents a correction to Lighthill's solution. The accuracy of applying (4) directly to calculate the heat transfer depends upon the Prandtl number and the convergence of the sequence (4b). In the original paper [5], Chao has calculated an order of magnitude of ε, $d\varepsilon/dX$, $d^2\varepsilon/dX^2$, etc. for incompressible wedge flow and has shown that the sequence (4b) converges well for Prandtl numbers larger than 0.1. However, the order of magnitude for other types of flow geometries deserves some discussion. Let's consider the cross flow over a circular cylinder ($L = D$). Using Hiemenz's empirical equation for U_e,

$$\frac{U_e}{U_\infty} = 3.6314\left(\frac{x}{D}\right) - 2.1709\left(\frac{x}{D}\right)^3 - 1.5144\left(\frac{x}{D}\right)^5 \tag{6}$$

and the expression for τ_w calculated by the Blasius procedure [6] as

$$\tau_w = 3.0157(\rho\mu)^{1/2} U_\infty^{3/2}\left(\frac{D}{2}\right)^{-1/2} \times\left[1 - 0.3513\left(\frac{2x}{D}\right)^2 - 0.06765\left(\frac{2x}{D}\right)^4\right]\left(\frac{2x}{D}\right) \tag{7}$$

the data for each term of ε, $d\varepsilon/dX$, $d^2\varepsilon/dX^2$, $d^3\varepsilon/dX^3$, and $d^4\varepsilon/dX^4$ are calculated for various values of x/D. For the isothermal surface, i.e. $x_0/D = 0$, and for $0.145 \leqslant x/D \leqslant 0.642$, the magnitudes of these terms are $0.7676 \leqslant |\varepsilon| \leqslant 0.4006$, $0.0096 \leqslant |d\varepsilon/dX| \leqslant 18.8791$, $0.0146 \leqslant |d^2\varepsilon/dX^2| \leqslant 579.05$, $5.0650 \leqslant |d^3\varepsilon/dX^3| \leqslant 18255.27$, and $8.9886 \leqslant |d^4\varepsilon/dX^4| \leqslant 991916.63$, respectively, and thus the sequence (4b) diverges. Under this condition, it was suggested by Professor Chao [7] that the Euler technique [8] must be applied to sum the sequence. To this end, it must be rearranged to properly order the terms as

$$-\frac{\partial\theta}{\partial\xi}(X,0) = 1.11985 + \underbrace{\left[-0.188868\varepsilon - 0.05731\frac{d\varepsilon}{dX} + 0.09861\frac{d^2\varepsilon}{dX^2} - 0.11358\frac{d^3\varepsilon}{dX^3} + 0.12004\frac{d^4\varepsilon}{dX^4} + \ldots\right]}_{S_1}$$
$$+ \underbrace{\left[-0.07271\varepsilon^2 - 0.03600\varepsilon\frac{d\varepsilon}{dX} + 0.09161\varepsilon\frac{d^2\varepsilon}{dX^2} - 0.10676\varepsilon\frac{d^3\varepsilon}{dX^3} + 0.10557\varepsilon\frac{d^4\varepsilon}{dX^4} + \ldots\right]}_{S_2}$$
$$+ \underbrace{[-0.05079\varepsilon^3 + \ldots]}_{S_3} \tag{8}$$

and S_1, S_2 and S_3 in (8) may be individually summed using the Euler technique. The required $-\partial\theta/\partial\xi\,(X, 0)$ is then given by $1.11985 + S_1 + S_2 + \ldots$, which may again be summed by the Euler technique if the above sequence diverges. However, for $x/D > 0.388$, it is not possible to obtain a reasonable result for the cross flow over a cylinder with the available terms provided in (8). Similar difficulty is encountered for the case of a step change in wall temperature for $x/D > 0.548$. Even for a large value of the Prandtl number, the convergence of S_1 and S_2, etc., in (8) cannot be improved since the order of ε is $Pr^{-1/3}$, and, therefore, the relative magnitudes of ε, $d\varepsilon/dX$, $d^2\varepsilon/dX^2, \ldots$, etc., in S_1 and ε^2, $d\varepsilon/dX, \ldots$, etc., in S_2 are the same. In order to improve the convergence of (4b), Chao [5] has expanded τ_w, ε, $\varepsilon^2, \ldots, d\varepsilon/dX, \ldots$, etc., in (4a,b) into powers of $2x/D$ and rearranged the sequences into a series of descending powers of the Prandtl number where the coefficients comprise ascending power series of $2x/D$. In the evaluation of the coefficients of the $2x/D$, $(2x/D)^2, \ldots$, etc., terms appearing in the latter series, various sums are obtained which consist of positive and negative terms which require Euler's summation technique to be applied when the sequence is not converging. In this way, Chao obtained an expression for $NuRe_D^{-1/2}$ for a circular cylinder, i.e. equation (63) in [5]. The numerical data obtained using this equation are also included in Table 1. Obviously this expression is much simpler to use and gives better convergence over the original expression (4a,b). Unfortunately, for non-isothermal surface temperatures, a similar expansion cannot be achieved since the series consists of descending and ascending powers of $2x/D$. However, for wedge flow with a step change in surface temperature, Chao has obtained a different type of series expansion from (4a,b) in [5].

In this paper, a totally different solution method is pursued for analyzing the heat transfer through an incompressible laminar boundary layer for two-dimensional and axisymmetrical bodies with non-isothermal wall temperature. The restriction of the one term or two term velocity distribution used in Lighthill's or Chao's analysis is relaxed. The analysis begins with the consideration of a step discontinuity in surface temperature and the solutions are expressible in series of appropriate transform variables with coefficients which are expressible as universal functions. The present analysis not only leads to the heat-

Table 1. Comparison of local Nusselt number $NuRe_D^{-1/2}$ for an isothermal circular cylinder, $Pr = 0.7$. Based on $U_e/U_\infty = 3.6314(x/D) - 2.1709(x/D)^3 - 1.5144(x/D)^5$. ϕ = angular displacement from front stagnation point

ϕ degree	Wedge variable Λ	x/D	a	a'	$NuRe_D^{-1/2}$: Present analysis equation (46a,b)	Present analysis equation (46a,b) with $a' = 0$, $a = a_0$	Frössling [13]	Chao and Fagbenle equation (34) in [9] or equation (48)	Chao equation (63) of [5]	Merk equation (42) of [10] or equation (47a,b)	Lighthill equation (29) of [1] or equation (1) with $x_0 = 0$
0	1.0	0	1.2326	0	0.9274(−1.8)†	0.9274(−1.8)†	0.9449	0.9450	0.9286	0.9406	1.1180
16.2	0.98	0.145	1.2227	−0.2787	0.9144(−2.09)	0.9172(−1.7)	0.9339	0.9339	0.9182	0.9300	1.1035
25.3	0.95	0.221	1.2079	−0.3236	0.8957(−2.49)	0.9029(−1.7)	0.9186	0.9186	0.9038	0.9151	1.0830
34.2	0.90	0.298	1.1831	−0.4093	0.8681(−2.98)	0.8809(−1.55)	0.8949	0.8948	0.8814	0.8922	1.1509
44.5	0.80	0.388	1.1326	−0.6245	0.8422(−1.40)	0.8427(−1.35)	0.8546	0.8542	0.8425	0.8521	0.9943
55.9	0.60	0.488	1.0216	−0.9381	0.7748(−1.88)	0.7784(−1.78)	0.7897	0.7925	0.7756	0.7846	0.8953
62.8	0.40	0.548	0.9282*	−1.2219	0.7257*(+0.21)	0.7212(−0.41)	—	0.7242*	0.7169	0.7244	0.8069
67.5	0.20	0.589	0.8397*	−2.8523	0.6724*(+2.50)	0.6657(+1.48)	—	0.6560*	0.6648	0.6660	0.7262
71.3	0.0	0.622	0.6241*	−4.0600	0.5772*(−4.67)	0.5996(−0.98)	—	0.6055*	0.6131	0.5965	0.6428

*Euler summation.
†Values in parentheses indicate percentage difference compared to data obtained from Merk's series of Chao and Fagbenle [9].

transfer characteristics but also to the temperature in the boundary layer downstream of the temperature discontinuity. The general solution to the problem is obtained and numerical examples are given for a circular cylinder of uniform and non-uniform surface temperature in cross flow. The present results are then compared with those obtained by using Lighthill's, Spalding's and Chao's formulae. The accuracy of the present method is also discussed. It is shown that the present formula provides a convenient and rapid procedure for calculating the heat-transfer rate across an incompressible laminar boundary layer for arbitrary distributions of main stream velocity and surface temperature.

2. THE PROBLEM AND ITS MATHEMATICAL FORMULATION

The physical system under investigation is illustrated in Fig. 1 for a two-dimensional or axisymmetric object of arbitrary shape which is situated in an incoming stream having a constant free stream velocity of U_∞ and an undisturbed isothermal temperature of T_∞. The flow is assumed to be steady and

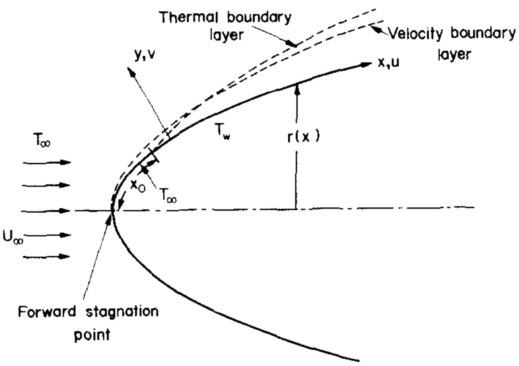

FIG. 1. Physical model and coordinate system.

incompressible and the free stream Mach number is sufficiently small for viscous dissipation effects to be neglected. The main effort in the present analysis is centered on the case where the wall temperature has a step change, i.e. a front portion of the object measured from the forward stagnation point to an arbitrary distance, x_0, is isothermal and possesses the free stream temperature value of T_∞, and for $x > x_0$, the wall temperature has a step change to T_w.

The governing boundary-layer energy equation for the problem under consideration is

$$u\frac{\partial T}{\partial x} + v\frac{\partial T}{\partial y} = \alpha\frac{\partial^2 T}{\partial y^2} \quad (9)$$

with the boundary conditions

$$\begin{aligned} T(x, 0) &= T_\infty + (T_w - T_\infty)I(x - x_0) \\ T(x_0, y > 0) &= T_\infty \\ T(x, \infty) &= T_\infty \end{aligned} \quad (10)$$

where $I(x - x_0)$ is the Heaviside unit operator and has the following values: for $x - x_0 < 0$, $I(x - x_0) = 0$; and for $x - x_0 \geqslant 0$, $I(x - x_0) = 1$.

To obtain the solution to (9), the velocity components u and v are assumed to be known. By using coordinate transformations for x and y [10] defined by

$$\left.\begin{aligned} x \to \xi &= \int_0^x \frac{U_e}{U_\infty}\left(\frac{r}{L}\right)^{2i}\frac{\mathrm{d}x}{L} \\ y \to \eta &= \left(\frac{Re_L}{2\xi}\right)^{1/2}\frac{U_e}{U_\infty}\left(\frac{r}{L}\right)^{i}\frac{y}{L} \end{aligned}\right\} \quad (11)$$

the velocity components can be written in terms of a dimensionless stream function, f, as

$$\frac{u}{U_e} = \frac{\partial f}{\partial \eta} \quad (12)$$

$$\frac{v}{U_e} = -(2\xi Re_L)^{-1/2}\left(\frac{r}{L}\right)^{i} \times\left\{f+2\xi\frac{\partial f}{\partial \xi}+\left(\Lambda+\frac{2\xi}{r}\frac{\mathrm{d}r}{\mathrm{d}\xi}-1\right)\eta\frac{\partial f}{\partial \eta}\right\} \quad (13)$$

where Λ is the "wedge variable" defined by

$$\Lambda = \frac{2\xi}{U_e}\frac{\mathrm{d}U_e}{\mathrm{d}\xi}. \quad (14)$$

In the above, $i = 0$ for two-dimensional flow and $i = 1$ for axisymmetric flow, and r is the body radius measured from the axis of symmetry. The dimensionless stream function f satisfies the transformed momentum equation,

$$\frac{\partial^3 f}{\partial \eta^3}+f\frac{\partial^2 f}{\partial \eta^2}+\Lambda\left[1-\left(\frac{\partial f}{\partial \eta}\right)^2\right] = 2\xi\left[\frac{\partial f}{\partial \eta}\frac{\partial^2 f}{\partial \eta\partial \xi}-\frac{\partial^2 f}{\partial \eta^2}\frac{\partial f}{\partial \xi}\right] \quad (15a)$$

which is subject to the boundary conditions

$$\left.\begin{aligned} f = 0,\ \frac{\partial f}{\partial \eta} &= 0, \ \text{for} \ \eta \to 0 \\ \frac{\partial f}{\partial \eta} &= 1, \ \text{for} \ \eta \to \infty. \end{aligned}\right\} \quad (15b)$$

The solution of (15) was first proposed by Merk [10] in series form and later refined by Chao and Fagbenle [9] as follows:

$$f(\xi,\eta) = f_0(\Lambda,\eta)+2\xi\frac{\mathrm{d}\Lambda}{\mathrm{d}\xi}f_1(\Lambda,\eta) +4\xi^2\frac{\mathrm{d}^2\Lambda}{\mathrm{d}\xi^2}f_2(\Lambda,\eta)+\left(2\xi\frac{\mathrm{d}\Lambda}{\mathrm{d}\xi}\right)^2 f_3(\Lambda,\eta) +\left(2\xi\frac{\mathrm{d}\Lambda}{\mathrm{d}\xi}\right)\left(4\xi^2\frac{\mathrm{d}^2\Lambda}{\mathrm{d}\xi^2}\right)f_{1,2}(\Lambda,\eta)+\ldots. \quad (16)$$

The solution to the energy equation (9) for the isothermal surface temperature case was also attempted by the above mentioned authors. Introducing the dimensionless temperature function defined by

$$\theta(\xi,\eta) = \frac{T-T_w}{T_\infty-T_w} \quad (17)$$

and using the similar transformation variables (11), the energy equation transforms to

$$\frac{\partial^2\theta}{\partial \eta^2}+Pr\cdot f\cdot\frac{\partial \theta}{\partial \eta} = 2Pr\xi\left[\frac{\partial f}{\partial \eta}\frac{\partial \theta}{\partial \xi}-\frac{\partial f}{\partial \xi}\frac{\partial \theta}{\partial \eta}\right]. \quad (18)$$

A similar series expansion analogous to (16) was also proposed for θ in [9].

When the surface condition has a step change as given by (10), the transformation (11) used for the isothermal case is not appropriate. Therefore, we further introduce the following dimensionless transformations:

$$\xi \to X = \left[1-\left(\frac{\xi_0}{\xi}\right)^C\right]^{1/3} \quad (19a)$$

$$\eta \to \zeta = b(\xi)\frac{\eta}{X} \quad (19b)$$

in which C is a constant,

$$\xi_0 = \int_0^{x_0}\frac{U_e}{U_\infty}\left(\frac{r}{L}\right)^{2i}\frac{\mathrm{d}x}{L},$$

and b is a function which depends on ξ and will be determined later. The transformations (19a,b) are a generalization of the Chao–Cheema transformation [11] used in the analysis of forced convection in wedge flow with a step discontinuity in surface temperature. With the introduction of these coordinate transformations, it will be shown in this study that the analysis for wedge flow can be extended to the case of flow over any two-dimensional or axisymmetrical body of arbitrary shape.

Making use of (17) and (19a,b), the energy equation is transformed to the following form:

$$\frac{\partial^2\theta}{\partial \zeta^2}+\frac{Pr}{b}\left[X\left(f+2\xi\frac{\partial f}{\partial \xi}\right)+\frac{2C}{3b}\frac{(1-X^3)}{X}\zeta\frac{\partial f}{\partial \eta} -2\xi\frac{\mathrm{d}b}{\mathrm{d}\xi}\frac{X^2}{b^2}\zeta\frac{\partial f}{\partial \eta}\right]\frac{\partial \theta}{\partial \zeta}-\frac{2C}{3b^2}Pr(1-X^3)\frac{\partial f}{\partial \eta}\frac{\partial \theta}{\partial X} = 0 \quad (20)$$

with

$$\theta(X,0) = 1 \quad (21a)$$

$$\theta(X,\infty) = 0. \quad (21b)$$

The range of the variables are $0 \leqslant X \leqslant 1$ and $0 \leqslant \zeta < \infty$. When $\xi = \xi_0$, X becomes zero and $\zeta \to \infty$ due to the form chosen for (19b). Therefore the entrance condition $T(x_0, y > 0) = T_\infty$ given in (10) merges into the condition given by (21b).

For the isothermal surface, $\xi_0 = 0$ and $X = 1$. Under this condition, we may choose b as a constant and $\zeta = b\eta$. Since

$$\frac{\partial \theta}{\partial X} = \frac{\partial \theta}{\partial \xi}\frac{\partial \xi}{\partial X} = \frac{3X^2\xi}{C(1-X^3)}\frac{\partial \theta}{\partial \xi},$$

the last term of (20) becomes

$$-\frac{2CPr(1-X^3)}{3b^2}\frac{\partial f}{\partial \eta}\cdot\frac{3X^2}{C(1-X^3)}\xi\left.\frac{\partial \theta}{\partial \xi}\right|_{X\to 1} = -\frac{2Pr}{b^2}\cdot\frac{\partial f}{\partial \eta}\xi\frac{\partial \theta}{\partial \xi}$$

with $\mathrm{d}b/\mathrm{d}\xi = 0$. Equation (20) thus reduces to Merk's form (18). Investigation of (19a) and (20) reveals that the constant C may be arbitrarily chosen as long as it is a positive real number. In order that the numerical results of the universal functions reported in [11] be directly applicable in the present analysis, $C = \frac{3}{4}$ was chosen in the successive analysis.

3. SOLUTION METHOD AND RESULTS

To obtain the solution to (20) with boundary conditions (21a,b), we first expand f in a power series of the form

$$f(\xi,\eta) = \sum_{n=2}^{\infty} a_n(\xi)\frac{\eta^n}{n!} \tag{22}$$

in which the a_n's may be obtained by substituting (22) into (15a) and equating coefficients having the same power of η. By substituting $\eta = \zeta X/b$ into (22), the resulting f is given by

$$f = \frac{a}{2}\frac{\zeta^2}{b^2}X^2 - \frac{\Lambda}{3!}\frac{\zeta^3}{b^3}X^3 + \frac{(2\Lambda-1)a^2+2\xi aa'}{5!}\frac{\zeta^5}{b^5}X^5 + \frac{(4-6\Lambda)\Lambda a-4\xi\Lambda' a}{6!}\frac{\zeta^6}{b^6}X^6 + \frac{(6\Lambda-4)\Lambda^2+4\xi\Lambda'\Lambda}{7!}\frac{\zeta^7}{b^7}X^7 + \ldots \tag{23}$$

and

$$\frac{\partial f}{\partial \xi} = \frac{a'}{2}\frac{\zeta^2}{b^2}X^2 - \frac{\Lambda'}{3!}\frac{\zeta^3}{b^3}X^3 + \frac{2\Lambda' a^2+4\Lambda aa'+2\xi a'^2+2\xi aa''}{5!}\frac{\zeta^5}{b^5}X^5 + \frac{4\Lambda a' - 12\Lambda\Lambda' a - 4\xi\Lambda'' a - 4\xi\Lambda' a' - 6\Lambda^2 a'}{6!}\frac{\zeta^6}{b^6}X^6 + \ldots. \tag{24}$$

In (23) and (24), the primes denote differentiation with respect to ξ, and $a = a_2 = \partial^2 f/\partial\eta^2|_{\eta=0}$. Numerical values of a and its derivatives for various values of Λ may be evaluated from (16) using the data reported in [9].

The solution to (20) is then expanded in series form as

$$\theta = \sum_{n=0}^{\infty} \theta_n(\xi,\zeta)X^n \tag{25}$$

with

$$\theta_0(\xi,0) = 1;\ \theta_1(\xi,0) = \theta_2(\xi,0) = \ldots = 0 \tag{26a}$$

$$\theta_0(\xi,\infty) = \theta_1(\xi,\infty) = \theta_2(\xi,\infty) = \ldots = 0. \tag{26b}$$

Therefore the boundary conditions (21a,b) are satisfied.

The θ_n's appearing in (25) can be obtained from the solutions to a set of differential equations which result from substituting (23), (24) and (25) into (20) and equating the coefficients of like powers of X. These equations (for $n \geqslant 1$) depend on the Prandtl number and Λ explicitly, and therefore the following universal functions will be introduced for the θ_n's so that the solutions can be evaluated once and for all. Rewriting the θ_n's ($n \geqslant 1$) in terms of these universal functions, we have

$$\theta_1 = \frac{3\Lambda}{2ab}\bar{\theta}_1 \tag{27}$$

$$\theta_2 = \left(\frac{3\Lambda}{2ab}\right)^2\bar{\theta}_2 \tag{28}$$

$$\theta_3 = \left(\frac{3\Lambda}{2ab}\right)^3\bar{\theta}_{3,1} - \frac{1}{Pra^2}[(2\Lambda-1)a^2+2\xi aa']\bar{\theta}_{3,2} + \tfrac{3}{2}\xi\left(\frac{d}{d\xi}\ln a\right)\bar{\theta}_{3,3}\ldots \text{etc.} \tag{29}$$

In the above equations, we have defined the undetermined function $b(\xi) = [a(\xi)Pr/3!]^{1/3}$. By using these universal functions and repeating the same operation as described before, we find that θ_0 and the $\bar{\theta}_n$'s satisfy the following equations:

$$\theta_0'' + 3\zeta^2\theta_0' = 0 \tag{30}$$

$$\bar{\theta}_1'' + 3\zeta^2\bar{\theta}_1' - 3\zeta\bar{\theta}_1 = \zeta^3\theta_0' \tag{31}$$

$$\bar{\theta}_2'' + 3\zeta^2\bar{\theta}_2' - 6\zeta\bar{\theta}_2 = \zeta^3\bar{\theta}_1' - \zeta^2\bar{\theta}_1 \tag{32}$$

$$\bar{\theta}_{3,1}'' + 3\zeta^2\bar{\theta}_{3,1}' - 9\zeta\bar{\theta}_{3,1} = \zeta^3\bar{\theta}_2' - 2\zeta^2\bar{\theta}_2 \tag{33a}$$

$$\bar{\theta}_{3,2}'' + 3\zeta^2\bar{\theta}_{3,2}' - 9\zeta\bar{\theta}_{3,2} = \tfrac{3}{4}\zeta^5\theta_0' \tag{33b}$$

$$\bar{\theta}_{3,3}'' + 3\zeta^2\bar{\theta}_{3,3}' - 9\zeta\bar{\theta}_{3,3} = -3\zeta^2\theta_0'. \tag{33c}$$

The associated boundary conditions are, respectively, $\bar{\theta}_1(\xi,0) = \bar{\theta}_2(\xi,0) = \bar{\theta}_{3,1}(\xi,0) = \bar{\theta}_{3,2}(\xi,0) = \theta_{3,3}(\xi,0) = 0$ and $\theta_1(\xi,\infty) = \theta_2(\xi,\infty) = \bar{\theta}_{3,1}(\xi,\infty) = \bar{\theta}_{3,2}(\xi,\infty) = \bar{\theta}_{3,3}(\xi,\infty) = 0$. The primes appearing in these equations denote partial differentiation with respect to ζ. Equations (30)–(32) and (33a,b) are precisely the same as those given in [11] for wedge flow, and (33c) is the same as equation (38d) given in [12] for non-Newtonian wedge flow. Therefore, the results obtained for wedge flow can be directly applied for the present problem. Solutions for (30), (31) and (33c) can be obtained in closed form. They are

$$\theta_0 = 1 - \frac{\Gamma(\frac{1}{3},\zeta^3)}{\Gamma(\frac{1}{3})} \tag{34}$$

and its derivative at the surface is

$$\theta_0'(0) = -\frac{3}{\Gamma(\frac{1}{3})} = -1.1198; \tag{35}$$

$$\bar{\theta}_1 = \frac{1}{5\Gamma(\frac{1}{3})}\cdot\zeta[\Gamma(\tfrac{4}{3}) - \Gamma(\tfrac{4}{3},\zeta^3)] \tag{36}$$

and its derivative at the surface is

$$\bar{\theta}_1'(0) = \tfrac{1}{15}; \tag{37}$$

and

$$\bar{\theta}_{3,3} = -\frac{1}{2\Gamma(\frac{1}{3})}\zeta e^{-\zeta^3} \tag{38}$$

with its derivative at the surface being

$$\bar{\theta}_{3,3}'(0) = -\frac{1}{2\Gamma(\frac{1}{3})} = -0.18664. \tag{39}$$

Equations (32) and (33a,b) have not been solved in closed form and they were numerically integrated. The results for these universal functions are tabulated in Table 1 of [11]. For determination of the temperature profile, the data for these functions are required and the reader may refer to [11]. For the evaluation of the wall heat flux, the wall derivatives for these functions are required and for the convenience of the reader, they are reproduced here as $\bar{\theta}_2'(0) = 0.81748 \times 10^{-2}$, $\bar{\theta}_{3,1}'(0) = 0.17204 \times 10^{-2}$, and $\bar{\theta}_{3,2}'(0) = 0.20737 \times 10^{-1}$.

The dimensionless temperature (25) can be recast in these universal functions as:

$$\theta(\Lambda, \zeta, X) = \theta_0 + 3\Lambda(2a)^{-1}\left(\frac{3!}{Pra}\right)^{1/3}\bar{\theta}_1 X + \left(\frac{3\Lambda}{2a}\right)^2\left(\frac{3!}{Pra}\right)^{2/3}\bar{\theta}_2 X^2 + \Big\{81(4Pr)^{-1}\Lambda^3 a^{-4}\bar{\theta}_{3,1} - [(2\Lambda-1)a^2+2\xi a a']Pr^{-1}a^{-2}\bar{\theta}_{3,2} + 2(3)^{-1}\xi\left(\frac{\mathrm{d}}{\mathrm{d}\xi}\ln a\right)\bar{\theta}_{3,3}\Big\}X^3 + \ldots \quad (40)$$

and the local heat flux at the wall is

$$q_w = k(T_w - T_\infty)\left(\frac{Pra}{3!}\right)^{1/3}\left(\frac{r}{L}\right)^i U_e X^{-1} \times (2\nu U_\infty L\xi)^{-1/2}\left(-\frac{\partial\theta}{\partial\zeta}\right)_{\zeta=0} \quad (41a)$$

where

$$\left(-\frac{\partial\theta}{\partial\zeta}\right)_{\zeta=0} = 1.1198 - 0.1\Lambda a^{-1}\left(\frac{3!}{Pra}\right)^{1/3} X - 0.81748(10^{-2})\left(\frac{3\Lambda}{2a}\right)^2\left(\frac{3!}{Pra}\right)^{2/3} X^2 - \Big\{0.34838(10^{-1})\Lambda^3 Pr^{-1}a^{-4} - 0.20737(10^{-1})Pr^{-1}a^{-2} \times [(2\Lambda-1)a^2+2\xi a a'] - 0.12442\xi\frac{\mathrm{d}}{\mathrm{d}\xi}\ln a\Big\}X^3 + \ldots. \quad (41b)$$

With the available information for a, a' and the universal functions θ_0 and $\bar{\theta}_i (i \geq 1)$, the evaluation of the temperature field and the local wall heat flux for flow with an arbitrary longitudinal pressure gradient using (40) and (41a,b) becomes a matter of arithmetic, which now proceeds as follows. For a given body, r and U_e are known functions of x (the dependence of U_e on x can be calculated from potential theory or derived from experiments), so that for each value of x the quantities ξ, Λ, $\mathrm{d}\Lambda/\mathrm{d}\xi$, etc., can be calculated. Hence, for each value of x, the corresponding values of a and a' can also be determined from tables or diagrams or equations in [9, 10]. Therefore, with specified x_0 and Pr, the temperature field and the local wall heat flux are rapidly calculated from (40) and (41a,b), respectively. As one can see from the derivation of these equations, no approximations or limitations have been imposed and therefore they are exact. With straightforward numerical integration of the higher order terms of the θ_n's in (25), we may readily provide more terms in the series solution in (40) and (41a,b) such that the higher order terms in the velocity distribution (23) can be properly accounted for in the solution to the energy equation. The accuracy of (40) and (41a,b) by using a finite number of terms in the series provided in this paper depends largely on the convergence of the series, i.e. Prandtl number and the range of X. For small Pr and $X \sim 1$, the series may become semi-divergent and Euler's summation method may be used. For a large Prandtl number or in the region close to the point of surface temperature discontinuity, the thermal boundary-layer thickness is comparatively much thinner than that of the velocity boundary-layer so that a linear velocity distribution may be used for the solution of the energy equation as done by Lighthill. This is the case $f = (a/2)(\zeta^2/b^2)X^2$ [retain only one term in (23)]. By substituting this velocity profile into (20), and performing a similar manipulation as before, the temperature field results as

$$\theta_l = \theta_0 + \tfrac{2}{3}\xi\frac{\mathrm{d}}{\mathrm{d}\xi}\ln a \cdot \bar{\theta}_{3,3}X^3 + \ldots \quad (42)$$

where the subscription l denotes the solution for a linear velocity profile. The corresponding wall heat flux is

$$(q_w)_l = k(T_w - T_\infty)\left(\frac{Pra}{3!}\right)^{1/3} \times \left(\frac{r}{L}\right)^i U_e X^{-1}(2\nu U_\infty L\xi)^{-1/2} \times \left[1.1198 + 0.12442\xi\frac{\mathrm{d}}{\mathrm{d}\xi}\ln a \cdot X^3 + \ldots\right]. \quad (43)$$

These two expressions can also be obtained from (40) and (41) by simply letting $Pr \to \infty$. In view of this, the solution of the energy equation using the linear velocity distribution is indeed an asymptotic solution for large Pr. The direct comparison of (43) for a two-dimensional body, $i = 0$, with Lighthill's result (1) cannot be achieved since they contain different parameters and coordinates. By comparing equations (42) and (43) with (40) and (41a,b), the excess terms appearing in the latter equations are obviously due to the contribution of the second and third terms of the velocity distribution in (23), and they are the correction terms to the linear velocity solution. It is therefore concluded that equation (41a,b) is applicable over a much wider range of parameters than Lighthill's equation (1). The application of the present formula to special cases and a comparison with the calculations obtained from other sources will be made in the next section.

4. APPLICATION OF THE GENERAL FORMULA TO SPECIAL CASES AND THE DISCUSSION OF ACCURACY

4.1. *Wedge flow*

Consider forced convection wedge flow in which there is a step discontinuity in wall temperature. Under this condition, the velocity distribution at the edge of the boundary layer is

$$U_e = Kx^{\beta/(2-\beta)}, \quad \text{and} \quad \Lambda = \beta, \quad a' = 0,$$

$$\xi = \frac{1}{U_\infty L}\frac{2-\beta}{2}U_e x, \quad i = 0.$$

Therefore, equation (41a,b) reduces to

$$\frac{q_w}{C_p \rho U_e (T_w - T_\infty)} = \frac{C_f}{2} Pr^{-2/3}(3!a^2)^{-1/3}X^{-1/3}\left(-\frac{\partial\theta}{\partial\zeta}\right)_{\zeta=0} \quad (44a)$$

where

$$\frac{C_f}{2} = \left(\frac{1}{2-\beta}\cdot\frac{v}{U_e x}\right)^{1/2} a$$

and

$$\left(-\frac{\partial\theta}{\partial\zeta}\right)_{\zeta=0} = 1.1198 - \frac{\beta}{10a}\left(\frac{3!}{Pra}\right)^{1/3} X - 0.81748\times 10^{-2}\left(\frac{3\beta}{2a}\right)^2\left(\frac{3!}{Pra}\right)^{2/3} X^2 - \left(0.34838\times 10^{-1}\frac{\beta^3}{Pra^4} + 0.20737 \times 10^{-1}\frac{(1-2\beta)}{Pr}\right)X^3 + \ldots \quad (44b)$$

with

$$X = \left[1 - \left(\frac{x_0}{x}\right)^{3/2(2-\beta)}\right]^{1/3}.$$

Equation (44a,b) is precisely the Chao–Cheema equation obtained in [11]. The accuracy of this equation has been extensively discussed in [11] and will not be repeated here. For the flow over a semi-infinite plate ($\beta = 0$), the second and the third terms in (44b) vanish. In order to provide one more non-vanishing term in the series solution, Chao and Cheema evaluate θ_6 in (25). For this case (44) becomes

$$\frac{q_w}{C_p \rho U_\infty (T_w - T_\infty)} = 0.3024 Re_x^{-1/2} Pr^{-2/3} X^{-1}\left(-\frac{\partial\theta}{\partial\zeta}\right)_{\zeta=0} \quad (45a)$$

and

$$\left(-\frac{\partial\theta}{\partial\zeta}\right)_{\zeta=0} = 1.1198 - 0.20737\cdot 10^{-1} Pr^{-1} X^3 - Pr^{-1}(0.41502 - 0.10445 Pr^{-1}) \times 10^{-2} X^6 + \ldots \quad (45b)$$

where

$$X = \left[1 - \left(\frac{x_0}{x}\right)^{3/4}\right]^{1/3}.$$

4.2. *Application to the calculation of the local heat transfer with uniform surface temperature*

The formula derived for a step change in surface temperature (41a,b), may be simply reduced to the uniform surface temperature case by substituting $X = 1$. For this case, we define a local Nusselt number by

$$Nu = \frac{q_w L}{k(T_w - T_\infty)}$$

and the group $NuRe_L^{-1/2}$ is given by

$$NuRe_L^{-1/2} = (Pra)^{1/3}\left(\frac{r}{L}\right)^i\left(\frac{U_e}{U_\infty}\right)\xi^{-1/2}\left(-\frac{\partial\theta}{\partial\zeta}\right)_{\zeta=0} \quad (46a)$$

with

$$\left(-\frac{\partial\theta}{\partial\zeta}\right)_{\zeta=0} = 0.43575 - 0.07071\cdot\Lambda Pr^{-1/3}a^{-4/3} - 0.02362\Lambda^2 Pr^{-2/3}a^{-8/3} - \Big\{0.01354\Lambda^3 Pr^{-1}a^{-4} - 0.00807 Pr^{-1}a^{-2}[(2\Lambda-1)a^2 + 2\xi a a'] - 0.12442\xi\frac{d}{d\xi}\ln a\Big\} + \ldots \quad (46b)$$

Using the series inversion and the asymptotic expansion technique, Merk [10] obtained the expression for the zero order solution, i.e. ignoring the RHS of (18) for a similar problem as

$$NuRe_L^{-1/2} = (Pra)^{1/3}\left(\frac{r}{L}\right)^i\left(\frac{U_e}{U_\infty}\right)\xi^{-1/2}\left(-\frac{\partial\theta_0}{\partial\xi}\right)_{\xi=0} \quad (47a)$$

where

$$\left(\frac{\partial\theta_0}{\partial\xi}\right)_{\xi=0} = 0.4358 - 0.06672\Lambda Pr^{-1/3}a_0^{-4/3} - 0.02336\Lambda^2 Pr^{-2/3}a_0^{-8/3} - [0.01482\Lambda^3 a_0^{-4} - 0.00968(2\Lambda - 1)]Pr^{-1} + (\text{terms involving } Pr^{-4/3}) + \ldots \quad (47b)$$

The above equation (47a,b) is indeed a local similarity solution of the energy equation (18), and the value of a_0 is defined by $a_0 = f_0''(0)$. The f_0 is likewise a local similarity solution of the Momentum equation (15a,b). By examination of (46a,b) and (47a,b), it can be seen that if the terms containing a' are neglected in (46b), and a is evaluated by using the local similarity solution $f_0''(0)$, then our folmula is essentially identical with Merk's with a slight discrepancy in the numerical coefficients. The first term on the RHS of (46b) and (47b) are in exact agreement. It represents the contribution of the linear components of the velocity profile. The other terms are almost identical and only differ slightly in the numerical coefficient. In view of the fact that these two formulae are derived from entirely different procedures, their resemblance in expression is quite surprising. To illustrate the application and the accuracy of our formula, an example is given for the cross flow over a circular cylinder. The Hiemenz expression of U_e (6) is again used for the calculation. The diameter of the cylinder, D, is now used for the characteristic length L, and $i = 0$ in (46a,b). The computed Nusselt numbers expressed as $NuRe_D^{-1/2}$ are summarized in Table 1 for $Pr = 0.7$. The numerical values of a and a' used in the calculation were obtained from the information given in [9]. The value of a was evaluated using the four term Merk's series, and the value of a' was obtained by Taylor's non-uniform interpolation method. These values are included in Table 1 for reference.

By refining Merk's series, Chao and Fagbenle [9] reported the results of the Nusselt number {equation (34) of [9]} as

$$NuRe_D^{-1/2} = \left(\frac{r}{D}\right)^i \frac{U_e}{U_\infty}(2\xi)^{-1/2} \times \left[\theta_0'(\Lambda,0) + 2\xi\frac{d\Lambda}{d\xi}\theta_1'(\Lambda,0) + 4\xi^2\frac{d^2\Lambda}{d\xi^2}\theta_2'(\Lambda,0) + \left(2\xi\frac{d\Lambda}{d\xi}\right)^2\theta_3'(\Lambda,0)+\ldots\right]. \quad (48)$$

By using the data for θ_n's $(\Lambda, 0)$ reported in [9], we have employed (48) to calculate $NuRe_D^{-1/2}$ for a circular cylinder. The results are also included in Table 1 for comparison. The data obtained from other sources as indicated are also included in this table. The results of Frössling [13] are usually considered exact up to $x/D = 0.45$. Data obtained from [9] are very close to these values for this range of x/D and, therefore, these data will be used as a standard for comparison for other values of x/D. Our data, in general, underestimate the Nusselt number except for values at $x/D = 0.548$ and 0.589, with a maximum difference of −4.67% occurring at $x = 0.622$. For other values of x/D, the differences are less than ±3%. When the Prandtl number increases, the agreement is expected to become better.

Equation (41a,b) may be used for engineering applications by ignoring a' in (41b) and using the similarity solution a_0 for a. Since the a' appears starting at the fourth term of the series, the error introduced by ignoring this term is expected to be small. With these approximations, the values of $NuRe_D^{-1/2}$ are calculated and are also shown in Table 1. Surprisingly, these values are closer to Chao and Fagbenle's data as compared to the values obtained by including the a' terms, with a deviation of less than 1.8% occurring for the range of x/D studied. This behavior may be due to the fact that, with these approximations, the sequence (41b) has better convergence for the four terms used in the present calculation. From Table 1, it can be seen that our data with $a' = 0$ are very close to those obtained using equation (63) of [5]. However, if (4a,b) is used for the calculation, the maximum deviation is 10.9% compared to Chao and Fagbenle's data for the range $0 \leqslant x/D = 0.388$, and for $x/D > 0.388$, additional terms in the sequences (4b) are required in order to obtain a reasonable result. As also shown in Table 1, Lighthill's formula overestimates the local Nusselt number. It is obvious that our equation (46a,b) offers an improvement to both Lighthill's (1) and Chao's (4a,b) formulae for isothermal surfaces.

4.3. *Application to forced convection over a circular cylinder in cross flow due to a step discontinuity in surface temperature*

For a non-isothermal surface condition, $X < 1$, and under this condition the convergence of the sequences $(-\partial\theta/\partial\zeta)_{\zeta=0}$ of (46b) becomes better compared to that of the isothermal case so that the accuracy of using finite terms in evaluating the heat transfer shall be improved. By employing the same mainstream velocity distribution and shear stress as for the isothermal case, we evaluated $NuRe_D^{-1/2}$ from Lighthill's (1), Spalding's (2), Chao's (4a,b) and our formula,

$$NuRe_D^{-1/2} = 0.38914(Pra)^{1/3}\left(\frac{r}{L}\right)^i \times \frac{U_e}{U_\infty}X^{-1}\zeta^{-1/2}\left(-\frac{\partial\theta}{\partial\zeta}\right)_{\zeta=0} \quad (49)$$

in which $(-\partial\theta/\partial\zeta)_{\zeta=0}$ is given by (41b). These results are tabulated in Table 2 for $Pr = 0.7$ and for x_0/D

Table 2. Comparison of $NuRe_D^{-1/2}$ for non-isothermal cylinder, $Pr = 0.7$, $x_0/D = 0.145$

			$NuRe_D^{-1/2}$			
ϕ degree	Wedge variable Λ	x/D	Present analysis (49)	Chao (4a,b)	Spalding (3)	Lighthill (1)
16.2	0.98	0.145	∞	∞	∞	∞
25.3	0.95	0.221	1.2211	1.1963*	1.25	1.3991
34.2	0.90	0.298	1.0328*	1.0620*	1.07	1.2114
44.5	0.80	0.388	0.9318*	0.9676*	0.970	1.0891
55.9	0.60	0.488	0.8313*	0.7707*	0.866	0.9550
62.8	0.40	0.548	0.7699*	†	0.786	0.8527
67.5	0.20	0.589	0.7111*	†	0.732	0.7639
71.3	0.00	0.622	0.6111*	†	0.675	0.6741

* Euler summation.
† More terms in (4a,b) are required in order to apply Euler summation technique.

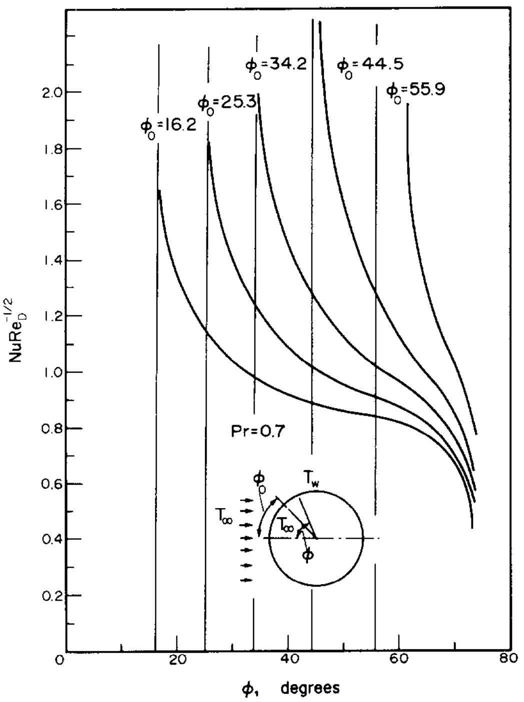

FIG. 2. Theoretical values of local Nusselt numbers for a cylinder with a step discontinuity in wall temperature at various ϕ_0, $Pr = 0.7$.

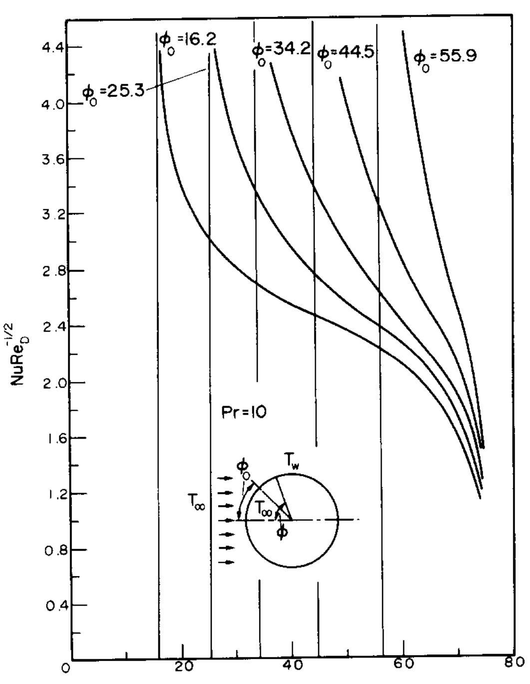

FIG. 3. Theoretical values of local Nusselt numbers for a cylinder with a step discontinuity in wall temperature at various ϕ_0. $Pr = 10$.

= 0.145. To the authors knowledge, no exact numerical data are available in the literature, so that a comparison can only be made among these four sets of data. Chao's data were obtained by Euler's summation as described in the introductory section and we are unable to obtain values for $\phi \geq 62.8°$. In the evaluation using Spalding's formula, the value of the correction function F was read from Fig. 2 of [4] and one iteration procedure was used. Spalding's data are closest to ours for the whole range of x/D. The local Nusselt numbers calculated from the present formula are summarized in Figs. 2 and 3 for $Pr = 0.7$ and 10, respectively, as a function of ϕ for various values of x_0/D or ϕ_0.

5. CONCLUSIONS

By introducing the appropriate transformation, the temperature field and the local wall heat flux due to a step change in wall temperature for two-dimensional or axisymmetrical boundary-layer flow with arbitrary pressure gradient can be expressed explicitly in terms of the Prandtl number and the wedge parameter. A great advantage of the present method is that one can refine the solution by obtaining more terms in the series in a straight-forward way to take into account more terms in the velocity profile. The equation obtained for a step discontinuity in wall temperature may directly be applied for a uniform wall temperature and for any arbitrary wall temperature simply by using Duhamel's theorem.

It is recommended that for engineering calculations, the term a' may be neglected in the expression for $(-\partial\theta/\partial\zeta)_{\zeta=0}$ and the similarity solution a_0 may be used for a in the calculation without introducing a significant error. By using Merk's formula [10] or Table 1 of [11], our formula provides probably one of the most rapid calculation methods of the temperature field and the local wall heat flux for non-isothermal surface conditions as any yet presented in the literature.

Finally, we hope that the present paper will fulfill the suggestion put forward by Chao and Cheema that the *modus operandi* of their analysis used for wedge flow [11] could be extended to treat general two-dimensional and axisymmetrical boundary-layer flow.

Acknowledgement—The authors would like to express their sincere appreciation to Professor B. T. Chao of the University of Illinois at Urbana–Champaign for his encouragement and friendly advice during the course of this investigation.

REFERENCES

1. M. J. Lighthill, Contributions to the theory of heat transfer through a laminar boundary layer, *Proc. R. Soc.* **A202**, 359–377 (1950).
2. H. W. Liepmann, A simple derivation of Lighthill's heat transfer formula, *J. Fluid Mech.* **3**, 357–360 (1958).
3. E. M. Sparrow, The thermal boundary layer on a non-isothermal surface with non-uniform free stream velocity, *J. Fluid Mech.* **4**, 312–329 (1958).
4. D. B. Spalding, Heat transfer from surfaces of non-uniform temperature, *J. Fluid Mech.* **4**, 22–32 (1958).
5. B. T. Chao, An improved Lighthill's analysis of heat transfer through boundary layers, *Int. J. Heat Mass Transfer* **14**, 907–920 (1972).
6. H. Schlichting, *Boundary Layer Theory*, Chapter 9, 6th edn. McGraw-Hill, New York (1968).
7. B. T. Chao, Private communication (letter dated 19 February 1976).

8. D. Meksyn, *New Methods in Laminar Boundary-Layer Theory*, Chapter 7. Pergamon Press, Oxford (1961).
9. B. T. Chao and R. O. Fagbenle, On Merk's method of calculating boundary layer transfer, *Int. J. Heat Mass Transfer* **17**, 223–240 (1974).
10. H. J. Merk, Rapid calculations for boundary-layer transfer using wedge solutions and asymptotic expansions, *J. Fluid Mech.* **5**, 460–480 (1959).
11. B. T. Chao and L. S. Cheema, Forced convection in wedge flow with non-isothermal surfaces, *Int. J. Heat Mass Transfer* **14**, 1363–1375 (1971).
12. J. L. S. Chen and P. T. Radulovic, Heat transfer in non-Newtonian flow past a wedge with non-isothermal surfaces, *J. Heat Transfer* **95C**, 498–504 (1973).
13. D. B. Spalding and W. M. Pun, A review of methods for predicting heat transfer coefficients for laminar uniform-property boundary layer flows, *Int. J. Heat Mass Transfer* **5**, 239–245 (1962).

CONVECTION THERMIQUE POUR DES COUCHES LIMITES AVEC UN GRADIENT ARBITRAIRE DE PRESSION ET DES SURFACES NON ISOTHERMES

Résumé—La méthode de résolution introduite par Chao and Cheema dans l'étude de la convection forcée sur un coin avec une température non uniforme de surface a été généralisée pour traiter le cas général des couches limites bidimensionnelles et axisymétriques avec une température pariétale non uniforme. En introduisant une transformation appropriée, les équations pour le profil de température et le flux thermique pariétal et local peuvent être exprimées explicitement en fonction du nombre de Prandtl et du paramètre du dièdre, pour une discontinuité en échelon de la température de paroi. Des exemples numériques pour un cylindre à surface isotherme et aussi avec un changement échelon de température sont donnés et comparés avec des valeurs obtenues à partir d'autres formules déjà publiées.

KONVEKTIVER WÄRMEÜBERGANG DURCH GRENZSCHICHTEN MIT BELIEBIGEM DRUCKGRADIENTEN UND NICHT-ISOTHERMER OBERFLÄCHE

Zusammenfassung—Die von Chao und Cheema in ihrer Untersuchung der Keilströmung bei erzwungener Konvektion und ungleichmäßiger Oberflächentemperatur vorgestellte Lösungsmethode wurde erweitert, um zweidimensionale und achsensymmetrische Grenzschichtströmungen mit ungleichmäßiger Oberflächentemperatur allgemein behandeln zu können. Durch die Einführung geeigneter Transformationsvariablen können die Gleichungen für das Temperaturprofil und den örtlichen Wärmestrom an der Wand explizit in Gliedern der Prandtl-Zahl und des Keilparameters für eine stufenförmige Diskontinuität in der Wandtemperatur ausgedrückt werden. Für eine isotherme Oberfläche und für eine stufenförmige Änderung der Wandtemperatur werden numerische Beispiele für einen Kreiszylinder angegeben und mit Werten verglichen, die mit anderen in der Literatur verfügbaren Formeln erzielt wurden.

КОНВЕКТИВНЫЙ ПЕРЕНОС ТЕПЛА ЧЕРЕЗ ПОГРАНИЧНЫЙ СЛОЙ ПРИ ПРОИЗВОЛЬНОМ ГРАДИЕНТЕ ДАВЛЕНИЯ И НАЛИЧИИ НЕИЗОТЕРМИЧЕСКИХ ПОВЕРХНОСТЕЙ

Аннотация — Предложенный Чао и Чима метод решения для клиновидного вынужденного течения при неравномерной температуре поверхности обобщен на двумерные и осесимметричные течения в пограничном слое при неравномерной температуре поверхности. Введя соответствующие коэффициенты преобразования, уравнения для температурного профиля и локального теплового потока на стенке можно представить в явном виде через критерий Прандтля и параметр клина при ступенчатой неравномерности температуры стенки. Приведены численные примеры для изотермической поверхности и ступенчатого изменения температуры стенки круглого цилиндра и дано сравнение с расчетами по другим известным в литературе формулам.